Anal Bioanal Chem (2013) 405:451–465
DOI 10.1007/s00216-012-6351-6

REVIEW

Carbon nanostructured materials for applications in nano-medicine, cultural heritage, and electrochemical biosensors

F. Valentini · M. Carbone · G. Palleschi

Received: 31 January 2012 / Revised: 28 June 2012 / Accepted: 13 August 2012 / Published online: 13 October 2012

Abstract This review covers applications of pristine and functionalized single-wall carbon nanotubes (SWCNTs) in nano-medicine, cultural heritage, and biosensors. The physicochemical properties of these engineered nanoparticles are similar to those of ultrafine components of airborne pollution (UF) and might have similar adverse effects. UF may impair cardiovascular autonomic control (inducing a high-risk condition for adverse cardiovascular effects), cause mammalian embryo toxicity, and increase geno-cytotoxic risk. SWCNTs coated with a biopolymer, for example polyethylenimine (PEI), become extremely biocompatible, hence are useful for in-vivo and in-vitro drug delivery and gene transfection. It is also possible to successfully immobilize a human enteric virus on PEI/SWCNT composites, suggesting application as a carrier in non-permissive media. The effectiveness of carbon nanostructured materials in the cleaning, restoration, and consolidation of deteriorated historical surfaces has been widely shown by the use of carbon nanomicelles to remove black dendritic crust from stone surfaces. The nanomicelles, here, have the twofold role of delivery and controlled release of the cleaning agents. The high biocompatibility of functionalized SWCNTs with enzymes and proteins is a fundamental feature used in the assembly of electrochemical biosensors. In particular, a third-generation protoporphyrin IX-based biosensor has been assembled for amperometric detection of nitrite, an environmental pollutant involved in the biodeterioration and black encrustation of historical surfaces.

Keywords SWCNTs · Biopolymers · Nano-medicine · Biosensors · Electrochemistry · Cultural heritage

Published in the special issue *Analytical Science in Italy* with guest editor Aldo Roda.

Electronic supplementary material The online version of this article (doi:10.1007/s00216-012-6351-6) contains supplementary material, which is available to authorized users.

F. Valentini (✉) · M. Carbone · G. Palleschi
Dipartimento di Scienze e Tecnologie Chimiche, II Università Degli Studi di Roma Tor Vergata,
via della Ricerca Scientifica 1,
00133, Roma, Italy
e-mail: federica.valentini@uniroma2.it

Introduction

In the past few years, carbon nanomaterials, for example nanotubes (CNTs), nanofibers [1, 2], and, recently, graphene oxide nanoribbons (GO) have attracted much interest for a wide variety of applications, from industry to biomedicine [3–6] and it can be forecast that many people will soon come in contact with such materials both in workplaces and in the environment. Although possible consequences of CNTs and GO exposure on human health are largely unknown, harmful effects cannot be excluded. In fact, some characteristics of engineered nanomaterials (ENMs), for example their high surface-to-volume ratio, make them potentially more toxic than their micrometric counterparts [5]. In comparison with other ENMs, intrinsic properties of CNTs might increase their toxicity; the fiber-like shape and low solubility might indeed account for their high biopersistence [7], possibly having long-term adverse effects even after sporadic exposure. Furthermore, differences in the presence of contaminants retained during CNTs synthesis [8, 9] compared with other "metal free" carbon nanomaterial, the deliberate introduction of oxygenated chemical groups (functionalization) [10], the length [11, 12], or the presence of structural defects [13–15] may also affect their toxicity [16]. Although several in-vivo and in-vitro studies of the toxicity of ENMs have been performed in the past few years [17, 18], comprehensive knowledge of their effects is not yet available. Modulation of nanoparticle surfaces can

affect particle uptake, biological response, and biodistribution [19, 20]. For instance, the biopersistence of carbon nanotubes can be drastically reduced by functionalizing them. Functionalized water-soluble carbon nanotubes are not retained in any of the mononuclear phagocyte system organs and are rapidly cleared from the systemic circulation by renal excretion [21]. After every modification performed on nanoparticles, the biocompatibility of the particles must be assessed. Surface functionalization can be used to increase circulation time in blood or reduce non-specific distribution, or for specific targeting of tissues or cells by use of a targeting ligand [22]. Recently, Dai and colleagues [23] demonstrated that GO functionalized with poly(ethylene glycol) (PEG) delivers aromatic, water insoluble anticancer drugs into cells. Their intrinsic optical properties have also been used for cell imaging [24, 25]. Chen et al. [25] showed that doxorubicin hydrochloride (DXR) could be efficiently loaded on to GO by a simple non-covalent method. The loading ratio of GO could reach 200 %, much higher than that of other nanocarriers [26]. There are already several promising applications of nanomaterials in biomedicine: targeted drug delivery is one of the most intensively investigated areas of research, and use of nanomaterials for diagnostic purposes has already been used in biomedicine [25]. This review focuses on the nano-toxicity (in vitro and in vivo) of pristine and oxidized SWCNTs and their biocompatibility, after functionalization with biopolymers, for example polyethylenimine (PEI). Compatibility with several biological materials suggests interesting opportunities for gene transfection, new strategies for cleaning historical stone surfaces, and biosensor assembly.

In particular, we report here six case studies we conducted on several aspects and applications of SWCNTs and nano-fibers:

1. cardiac autonomic regulation after lung exposure;
2. low doses of pristine and oxidized single-wall carbon nanotubes in mammalian embryonic development;
3. study of the effects of single-wall carbon nanotubes on human cells in the oral cavity, including geno-cytotoxic risk;
4. investigation of the interaction between single-wall carbon nanotubes and a human enteric virus;
5. new strategies for cleaning deteriorated stone surfaces based on the use of carbon nanomicelles as carriers of cleaning agents; and
6. assembly of amperometric biosensors modified by use of carbon nanomaterial–hemin nanocomposite for direct electrochemical detection of environmental pollutants, for example nitrite and H_2O_2 (the latter for glucose biosensor development).

Each case study is subdivided into three sections: the material used, the results obtained, and discussion of the most important results.

Cardiac autonomic regulation after lung exposure to carbon nanotubes

Materials and procedures

An in-vivo study was performed on 13 adult Wystar–Kyoto (WKY) rats of both sexes (350 g body wt). Experimental procedures were in accordance with the Association for Assessment and Accreditation of Laboratory Care International and approved by the animal care facility (Stazione per la Tecnologia Animale) of the University "Tor Vergata" and by the Italian Health Minister [27]. SWCNT or PBS were given to SWCNT-instilled rats (n=8) and a control group (n=5), respectively, at time 0 and time 1, immediately after arterial pressure recording. Suspensions of carbon nanotubes were prepared by sonication in phosphate-buffered saline (0.1 $molL^{-1}$ PBS, pH 7.4) and ultrasonicated for at least 10 min before each instillation experiment. Dispersed SWCNTs were instilled intratracheally within 1 min after sonication, to ensure stability of the homogeneous SWCNT dispersion. The amount of SWCNT given during each session was 1 $\mu g kg^{-1}$ body weight [27].

Results

The effects of the SWCNT instillation was determined by the monitoring the arterial baroreflex control of the sinus node as index of cardiovascular autonomic control, because it has been widely implicated as an important negative prognostic index in predicting mortality from ischemic heart disease and myocardial infarction [27].

In particular, the occurrence of baroreflex sequences revealed an evident and significant trend to decreased response to SWCNT exposure whereas the number of baroreflex sequences did not change significantly in response to PBS instillations (Fig. 1). More important, this result was achieved with a relatively small amount of SWCNT. It was estimated that exposure of mice lungs to 0.5 μg SWCNT kg^{-1} body weight is equivalent to the exposure of workers handling SWCNT for 200 workdays, [27]. Correspondingly, the amount of SWCNT used in this study is approximately equivalent to workers' exposure during approximately 400 workdays, i.e. less than two years.

Evaluation of cardiovascular autonomic regulation and of the baroreflex control of the sinus node was

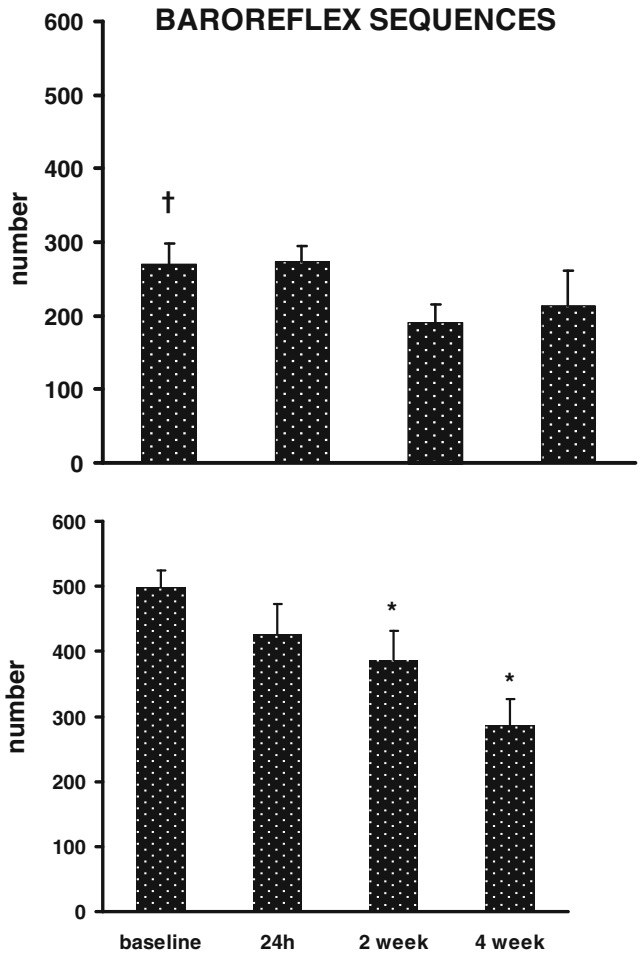

Fig. 1 Number of baroreflex sequences during instillation of PBS (controls, *upper panel*) and single-wall carbon nanotubes (SWCNT, *bottom panel*) at different times (see "Methods" section). Data are shown as mean±SEM. *$P<0.05$ vs baseline; †$P<0.05$ control vs SWCNT group baseline values

performed in a physiological setting without any external perturbations on the cardiovascular system. This is important, because external factors, for example drugs injection, anxiety because of restriction, and anesthetics can have a large effect.

Discussion

These results show that the ultrafine component (UF) of airborne pollution may impair cardiovascular autonomic control, a high-risk condition for adverse cardiovascular events. Because the physicochemical properties of engineered nanoparticles, for example single-wall carbon nanotubes (SWCNT), are similar to those of UF, they might have similar adverse effects. A significant decrease in the number of baroreflex sequences (from 502 at baseline to 194 at the post-four-week recording) was observed in SWCNT-instilled rats, whereas no significant change was detected in controls.

These data suggest that SWCNT may alter the BRF, thus affecting autonomic cardiovascular control regulation.

Low doses of pristine and oxidized single-wall carbon nanotubes in mammalian embryonic development

Materials and procedures

Six to eight-week-old females of CD1 outbred strain (Charles River, Calco, Italy) were used as a general multipurpose model for in-vivo studies. All procedures were approved by the Institutional Animal Care and Use Committee and complied with European rules (116/92.) All animals were housed and mated under standard laboratory conditions and their weight was between 30 and 35 g. Females at day 5.5 of gestation were injected in the retrobulbar plexus with nanosized carbon black (n-CB), and with pristine (p), oxidized (o), and ultra oxidized (uo) SWCNTs. Stock solutions contained 1 $mg mL^{-1}$ nanoparticles in controlled medium, i.e. 10 mg bovine serum albumin (BSA) and 1 mL Dulbecco's modified Eagle medium (DMEM) [28]. For in-vitro cell-culture experiments, mouse ES (embryonic stem) cell line D3 and NIH3T3 cells were purchased from ATCC (America Type Tissue Collection, Manassas, VA, USA). Both cell lines were maintained in culture by following standard procedures. For the mES cells the concentrations tested were 0.1, 1, 2, 6, and 10 $\mu g mL^{-1}$; for NIH3T3 cells 10 times higher concentrations were used. For mES cell differentiation into embryoid bodies the "hanging drops" procedure was followed, in accordance with the EST (embryonic stem cell test) guidelines [28]. Evaluation of oxidative stress on the basis of measurement of production of reactive oxygen species (ROS) was performed on tissue homogenates by conversion of nonfluorescent 20,70-dichlorofluorescein diacetate to the highly fluorescent 20,70-dichlorofluorescein [28].

Results

At 30 μg/mouse dose, all types of SWCNT, but not n-CB, were able to induce gross fetal morphological abnormalities (Table 1) [28]. A substantial percentage of SWCNT-exposed mice (ranging from 19 % to 31 %) had swollen uteri with no developed embryos (Table 1), a finding never observed in control females and which we interpreted as evidence of early miscarriages. With the objective of identifying the concentration of SWCNTs with no teratogenic or abortive effects, decreasing doses of the materials were used in subsequent experiments. Interestingly, at 3 μg/mouse the percentage of females with early miscarriages decreased substantially, but percentages of mothers with malformed fetuses increased (Table 1). At even lower dosages (0.3 and

Table 1 Summary of the percentage of females whose pregnancy was affected by exposure to different concentrations of three samples of SWCNTs

	30 μg/mouse				3 μg/mouse				0.3 μg/mouse				0.1 μg/mouse				0.01 μg/mouse			
	♀	A	B	A+B	♀	A	B	A+B	♀	A	B	A+B	♀	A	B	A+B	♀	A	B	A+B
CTRL	20	0	0	0	21	0	0	0	21	0	0	0	21	0	0	0	20	0	0	0
n-CB	23	0	2	0	18	0	0	0	18	0	0	0	20	0	0	0	20	0	0	0
p-SWCNTs	21	19	4.7	23.7	22	4.5	27.3	31.8	19	0	5.3	5.3	20	0	5	5	18	0	0	0
o-SWCNTs	20	20	20	40	21	4.8	9.5	14.3	20	0	5	5	18	0	5.5	5.5	18	0	0	0
uo-SWCNTs	16	31	25	56	20	0	45	45	16	0	18.7	18.7	23	0	8.7	8.7	20	0	0	0

♀, number of females analyzed in each group; A, percentage of ♀ with swollen uteri and no fetuses; B, percentage of ♀ with at least one malformed fetus

0.1 μg/mouse), no miscarriages were observed, but mothers carrying fetuses with gross malformations were still present, although numbers were much lower (Table 1). Finally, at a concentration of 0.01 μg/mouse no miscarriages or fetal malformations were observed (Table 1). At all dosages, n-CB or vehicle did not have any teratogenic or abortive effect [28]. A wide variety of malformations was found (Figs. 2a–h), but no differences in their type and severity were observed among the three groups of CNTs and among different concentrations within each group. In some cases the fetuses appeared morphologically normal, but significantly growth retarded (Fig. 2e); more often, fetuses with abdominal wall or head deformities or limb hypoplasia (Figs. 2b–d and f) were observed. In more abnormal fetuses, severe retardation in the development of several organs and tissues was associated with abnormal torsion of the trunk (Fig. 2g), or the body plan was profoundly affected and the outline of the fetus could be barely identified (Fig. 2h). In a small set of experiments, females were treated with low doses of SWCNTs (0.3 and 0.1 μg/mouse) at the peri-implantation stage (between days 4.5 and 5 of gestation). Interestingly, in p and uo-SWCNT-treated females, besides the presence of malformations, a few fetuses were found to share the same placenta (Figs. 2i and l). For 80 % of twins we observed intertwin discordance encompassing fetal size, feto-placental hemodynamics, and structural defects. Such features resemble vascular pathology that can complicate monochorial twin pregnancies in humans, for example the "twin to twin transfusion syndrome" and the "twin reversed arterial perfusion sequence" (Figs. 2i and l). In both complications one of the twins is developmentally retarded because of blood transfusion via placental vascular anastomosis between the two circulations [28]. Analysis of the gonads revealed that fetuses attached to the same placenta were always of the same sex, a further indication of monozygotic twinning. Monozygotic twinning is extremely rare in mice, and in mammals it is widely accepted that its occurrence is a consequence of teratogenic stimuli [28], thus indicating that the observed twins might be a result of the teratogenic effect of SWCNTs. No monozygotic twinning was ever observed in n-CB and vehicle-treated females.

In detail, obvious alterations in size and vascular organization of the labyrinth layer were observed for abnormal placentas (supplementary material Figs. S1 a–c), which were characterized by disruption of the radial distribution and arborization of the placental vascular bed. Immunohistochemical analysis using antibodies against the pan-endothelial marker CD31 (supplementary material Figs. S1d and e) and Azan–Mallory staining (supplementary material Figs. S1f and g) revealed strongly reduced vessel density and branching and areas of fibrin deposition, reflecting the presence of thrombotic vessels. The presence of extensive vascular alterations and of thrombi in our model system (supplementary material Fig. S1d–g) led us to hypothesize that placental damage might be a consequence of oxidative stress, induced by reactive oxygen species (ROS) [28].

In-vitro models for screening of nanomaterial embryotoxicity were also tested, because they are less expensive than the in-vivo counterparts and fewer ethical issues are involved. For this purpose, the reliability of the EST, a validated test for predicting embryotoxicity of chemical compounds [28], was performed in parallel with the in-vivo studies.

In the EST two stable cell lines are used—NIH3T3 fibroblasts, representing differentiated tissue, and mouse embryonic stem (mES) cells. In this experiment, the effect of SWCNTs on cell proliferation was studied by growing the cells in medium containing the same carbon compounds used in the in-vivo experiments [28]. After 10 days of culture, cell viability was measured by use of a colorimetric assay (WST-1) and half maximum inhibitory concentration (IC_{50}) values were calculated for each carbon compound for each cell line (supplementary material Fig. S2a and b). The

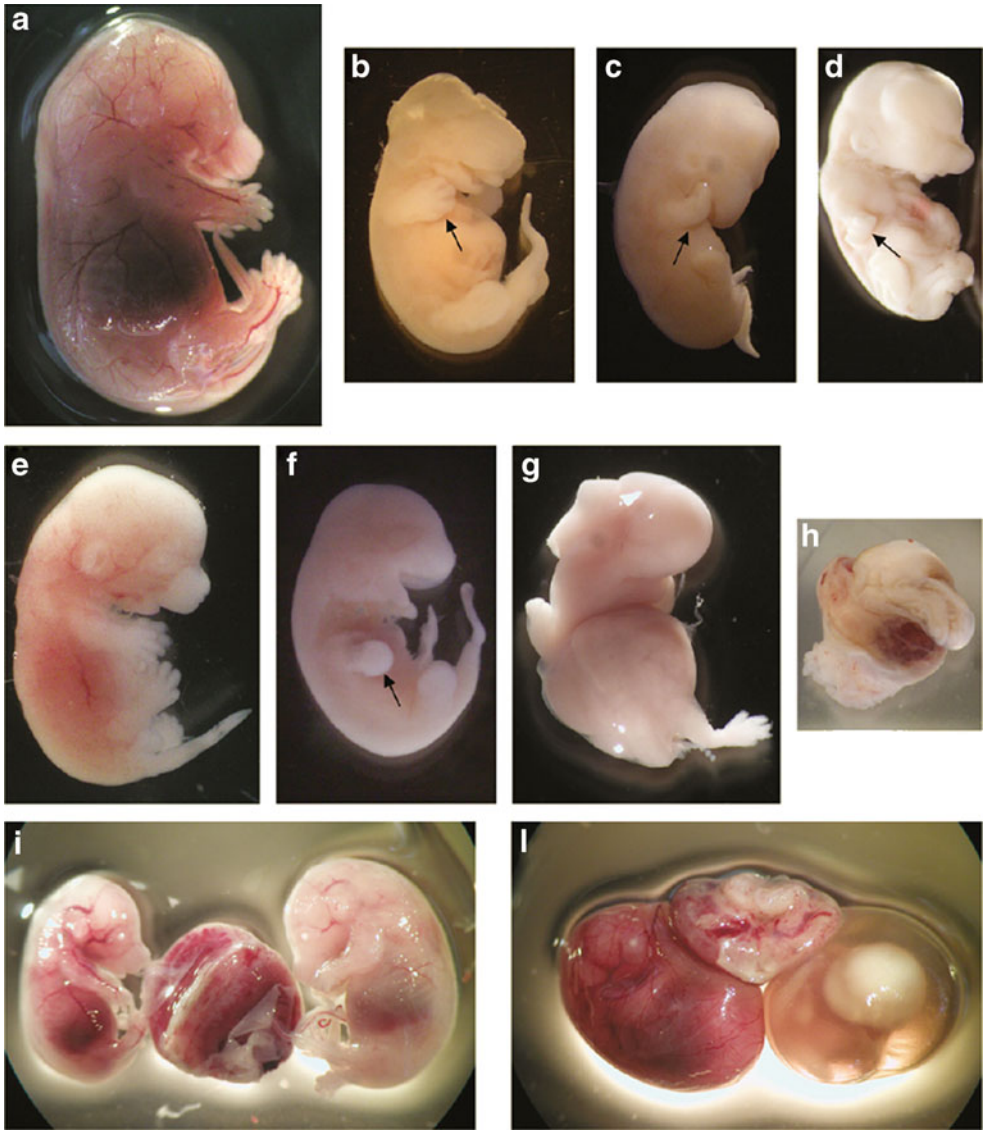

Fig. 2 Representative images of 15.5 dpc malformed fetuses from SWCNT-treated mothers. Images are of fetuses from mothers exposed to 0.3 μg/mouse, but similar phenotypes were observed for all other effective doses tested. **a** Normal fetus. **b**–**d** Malformed fetuses from (**b**) p, **c** o, and **d** uo-SWCNT-treated mothers. SWCNT-exposed fetuses appeared developmentally hindered compared with controls. *Arrows* indicate limbs that appear severely retarded in their development. **e**–**h** Irrespective of the type and dosage of SWCNT injected, fetuses with malformations of different severity were recovered. **e** Some fetuses, although smaller, appeared only slightly affected by the treatment, with an overall body plan comparable with that of normal fetuses. **f** Fetuses with more severely retarded development of the limbs and snout were observed. **g** In some cases fetuses were missing the crown–rump organization and appeared folded, with swollen abdomen. **h** Small abnormal placentas with very early developmentally arrested embryo were also recovered. **i**, **l** Two cases of monozygotic, diamniotic twin fetuses. **i** Twins appear morphologically normal but the fetus on the left side is significantly smaller. **l** The twin on the right side appears severely developmentally retarded. All photographs are at the same magnification

EST algorithm classified all three types of SWCNT as "strongly embryotoxic" [28].

Discussion

Several in-vitro and in-vivo studies suggest local and systemic effects after exposure to carbon nanotubes. No data are available, however, on their possible embryotoxicity in mammals. In this study, we tested the effect of pristine and oxidized single-wall carbon nanotubes (SWCNTs) on the development of the mouse embryo. A high percentage of early miscarriages and fetal malformations was observed for females exposed to oxidized SWCNTs; the percentage was lower for animals exposed to the pristine material. The lowest effective dose was 100 ng/mouse. Extensive vascular lesions and increased production of reactive oxygen species (ROS) were detected in the placentas of malformed fetuses but not of normally developed fetuses. Increased ROS levels

were, likewise, detected in malformed fetuses. No increased ROS production or evident morphological alterations were observed in maternal tissues. No fetal and placental abnormalities were ever observed in control animals. In parallel, SWCNT embryotoxicity was evaluated by use of the embryonic stem cell test (EST), a validated in-vitro assay developed for predicting the embryotoxicity of soluble chemical compounds, but never applied in full to nanoparticles. The EST predicted the in vivo data, identifying oxidized SWCNTs as the more toxic compounds.

Study of the effects of single-wall carbon nanotubes in human cells of the oral cavity: geno-cytotoxic risk

Materials

Oxidized single-wall carbon nanotubes, (o-SWCNTs) were dispersed (5 $\mu g mL^{-1}$) by direct ultrasonication, for 2 h, in culture medium containing 1 % FBS (fetal bovine serum) as the dispersion vehicle [29]. Immediately after preparation the o-SWCNT suspension was applied to human gingival fibroblasts. All treatments were performed on semiconfluent cultures exposed to 50, 75, 100, 125, or 150 $\mu g mL^{-1}$ o-SWCNTs for 24 h; control cells were treated with the same volume as that used to dissolve the compounds. After exposure to the different doses of o-SWCNTs, cells were treated for 6 h with 100 $\mu mol L^{-1}$ heat-shock factor (HSF) inhibitor *N*-formyl-3,4-methylenedioxybenzylidene butyrolactam (KNK437, Calbiochem) in DMSO [29]. The cytokinesis-block micronucleus (CBMN) test, comet assay, cytotoxicity assay, detection of cell death, and the ROS detection were performed in accordance with the procedures described in Ref. [29].

Results

The purpose of this study was investigation of the in-vitro effects of o-SWCNTs on cells of the oral cavity. For this purpose, human gingival fibroblasts were exposed to 50, 75, 100, 125, or 150 $\mu g mL^{-1}$ SWCNTs for 24 h and several tests were performed. Genotoxicity, cytotoxicity, oxidative stress, and stress response were investigated by use of the Comet assay, micronucleus test, by ROS generation (Fig. 3), and by heat-shock protein 70 (Hsp70) expression [29]. It was found that o-SWCNTs induced genotoxic effects at all doses, and at the two highest doses induced apoptosis also (supplementary material Fig. S3). Finally, by inhibition of Hsp70 expression, it was demonstrated that this heat-shock protein conferred protection against SWCNT geno-cytotoxicity, [29].

Discussion

Several studies have been performed to investigate the effects of carbon nanotubes on many human cell types, but to the best of our knowledge there are no reports of the action of SWCNT on human gingival fibroblasts (HGFs), even though they are of experimental interest because of their possible contact with the environment. It is a matter of fact that nanomaterials are able to cross the epithelial tissue, and so can, presumably, cross the gingival epithelium also, interacting with gingival fibroblasts [29]. In this work we examined the response of HGFs to carboxylated SWCNT treatment by analyzing the induction of DNA damage and cytotoxicity. We further investigated the ability of these nanomaterials to act as inducers of oxidative stress and stress response, by testing ROS production and Hsp70 expression. We therefore exposed HGFs to different doses of SWCNTs for 24 h. Our data on genotoxicity, obtained by use of the CBMN test and the alkaline Comet assay, clearly demonstrated that carbon nanotubes induced DNA damage. In the micronucleus test, an increase in chromosome damage was discovered up to 100 $\mu g mL^{-1}$ SWCNTs. Collapse of the number of micronuclei was observed at the two highest doses, significant relative to basal value. Levels of DNA damage assessed by the Comet assay were higher for all doses. These results are in accordance with those reported by Migliore et al., cited in Ref. [29], which found carbon nanotubes (1–100 $\mu g mL^{-1}$) increased DNA damage in murine macrophage cells tested by the CBMN test and Comet assay. Similar results have been reported for Chinese hamster lung fibroblasts, human mesothelial cells, and human bronchial epithelial cells (Ref. [29] and references cited therein). Cell proliferation and survival data were indicative of substantial decreases in cell growth and viability at the two highest concentrations, supporting the hypothesis that the MN collapse was because of severe DNA damage, as clearly demonstrated by the Comet assay. More specifically, analysis of the cell distribution by type of DNA damage showed a high percentage of cells were highly damaged at 125 and 150 $\mu g mL^{-1}$ and the presence of cells with maximum damage at the highest dose. It is well known that the DNA injury response is a critical moment in cell life, causing slowing of the cell cycle to enable DNA damage repair and apoptotic events if the damage is irreparable (Ref. [29] and references cited therein). In the HGF line, the crucial moment for cell survival seemed to be exposure to 100 $\mu g mL^{-1}$ nanotubes, as shown by the geno-cytotoxic data. Also the balance between oxidized and reduced compounds is important for cell life and a shift of this balance, oxidative stress, is usually associated with production of ROS. Our data on oxidative stress induction revealed that the SWCNTs caused an increase in the amount of ROS at all doses tested compared with the control value, confirming

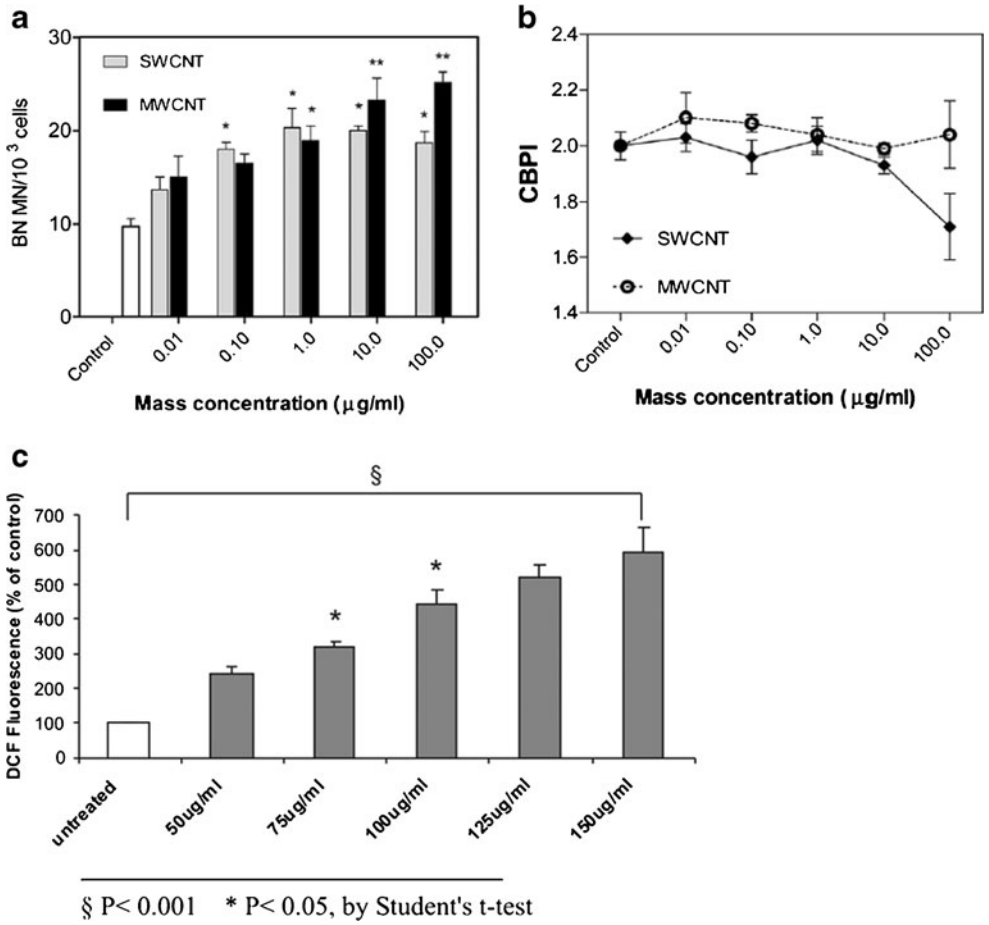

Fig. 3 Induction of ROS generation by SWCNTs in HGFs. Cells were treated with different concentrations (50, 75, 100, 125, and 150 $\mu g mL^{-1}$) for 24 h and ROS production was measured by analysis of DCF fluorescence compared with untreated cultures. Results are expressed as percentage of control and reported as mean± SE from four separate experiments for each experimental point. § Refers to comparison of treated and untreated cultures; * refers to comparison a dose and the previous dose

previous reports (Ref. [29] and references cited therein). The stress response was tested as Hsp70 expression. It is well known that heat-shock proteins, expressed at low levels under physiological conditions, can be induced by a wide variety of stressful stimuli, including many environmental stresses and ROS (Ref. [29] and references cited therein). We found that exposure to SWCNTs significantly induced Hsp70 expression, which reached the maximum level at 100 $\mu g mL^{-1}$ and persisted unchanged at the two highest doses. This finding suggested that high doses of SWCNT might affect Hsp70 induction. Analysis of the relationship between Hsp70 levels and DNA damage induced by various stressors is of interest for evaluation of possible involvement of HSPs in genotoxicity modulation. On this subject, there have been reports of a protective role of Hsp70 against DNA damage (Ref. [29] and references cited therein) and its involvement in the DNA repair system (Ref. [29] and references cited therein). In analysis of our data, comparison between Hsp70 expression and DNA damage induction measured by the Comet assay (which enabled detection of the damage at all doses) showed that Hsp70 levels increased in parallel to the tail moment values in a defined range of SWCNT exposure (50–100 $\mu g mL^{-1}$). At the two highest doses no further increment in Hsp70 expression was observed, whereas more DNA damage was found. Interestingly, at the same doses cytotoxicity, also, increased substantially, as demonstrated by results for cell vitality and cell death. There is plenty of evidence of the involvement of Hsp70 in regulation of apoptosis under stressful conditions (Ref. [29] and references cited therein) and Didelot et al. found that the Hsp70 expression levels are important in determining the fate of cells in response to stressful stimuli (reported in Ref. [29]). Because of these considerations and taking into account our data on cytotoxicity and Hsp70 expression, we supposed that the levels of Hsp70 observed for the highest doses of SWCNT (when levels of Hsp70 no longer increased) could not effectively counteract the damage, as shown by pronounced cell vitality decrease and apoptosis induction at these concentrations. This could mean that in the 50–100 $\mu g mL^{-1}$ range of exposure, where Hsp70 expression significantly increased, protein levels still had a protective effect, attenuating the injuries. Given this assumption, it is reasonable to expect this protective action against DNA damage also, at least in a defined range. If Hsp70 is, indeed, involved in protection against the effects of SWCNT, inhibition of its synthesis should result in a more extensive damage. Because the key event in heat shock response consists in activation of the HSF1

transcription factor, its inhibition leads to no expression of HSPs. KNK437, an inhibitor of HSF1, was chosen to demonstrate the actual protective role of Hsp70 against genocytotoxicity. These results showed that abrogation of Hsp70 induction increased the sensitivity of human gingival fibroblasts to the injuries caused by SWCNTs. The lack of Hsp70 expression led to a significant increase of DNA damage, as indicated by tail moment values at all doses of nanotubes and the appearance of the maximum damage class at 75 and 100 $\mu g mL^{-1}$. This finding provided strong evidence that the protein is involved in attenuation of the genotoxicity and it is consistent with the knowledge that Hsp70 function occurs at the DNA repair level. Furthermore, inhibition of Hsp70 expression also resulted in an increase of cytotoxicity, both as a decrease of cell viability and as apoptosis, confirming the well known evidence of the protective effect of Hsp70 on cell survival. However, the effect of the Hsp70 inhibitor was not evident when the cells were treated with 150 $\mu g mL^{-1}$ SWCNTs. We supposed that at this high dose of exposure, the extensive induced damage would have exceeded the protective capacity of Hsp70, so that inhibition of its synthesis would not have been critical for cell survival.

Interaction between single-wall carbon nanotubes and a human enteric virus

Materials

SCWNTs functionalized with 25-kDa PEI or carboxyl groups were dissolved in DMEM (Dulbecco's modified Eagle medium) containing 1 % FCS (fetal calf serum) [30, 31] at a final concentration of 1 $mg mL^{-1}$ by sonication in an ultrasonic bath for 2–3 h before each virus-based test. Different amounts of hepatitis A Virus (HAV), strain HM175 [30, 31], were added to this homogeneous and stable dispersion, and HAV was enabled to conjugate with the SCWNT–PEI and SCWNT–COOH at room temperature. The viral suspension at the indicated concentration in DMEM 1 % FCS (100 µL) was mixed in ice with 100 µL SCWNT–PEI or SCWNT–COOH at different concentrations. Virus detection was performed by reverse transcriptase polymerase chain reaction (RT-PCR), and virus titration by real-time polymerase chain reaction (qRT-PCR) [30, 31].

Results

Functionalized single-wall carbon nanotubes have been used for biomedical purposes as carriers for drugs, peptides, proteins, and nucleic acids. A large volume of data indicates their suitability to act as a carrier but only after coating with a biopolymer, for example polyethylenimine (PEI). The ability of two differently activated SWCNTs (with carboxyl groups or with carboxyl groups and polyethylenimine (PEI)) to form a complex with the hepatitis A virus was evaluated [30, 31]. Both types of activation enabled the formation of a virus–SWCNT complex (Fig. 4 and supplementary material Table S1). However, their patterns were different. The carboxyl-activated nanotubes had a somewhat low adsorptive capacity that was inversely related to the concentrations of the SCWNTs and viruses. The χ^2-test revealed there were no significant differences among SWNT–PEI 2.5, 1, and 0.5. However, significant differences were observed between SWNT–PEI 0.5, SWNT–PEI 0.2, and SWNT–COOH ($P<0.05$) [30, 31]. Addition of PEI improved the adsorption, probably because of the electropositive charge of the molecule, which interacts with the negatively charged virus of hepatitis A. Adsorption is optimum between 100 µg and 10 ng with an SCWNTs–PEI weight ratio of 1:0.2 up to an inoculum of 10^5 genome equivalents of hepatitis A virus, [30, 31]. Reducing or increasing this weight ratio reduced the adsorptive capacity of the PEI. Furthermore, this adsorption activity is time and contact-dependent. Thus, SCWNTs coated with PEI are able to complex with viruses, and may be tested to transfect non-permissive cell lines.

Discussion

The development of a nontoxic and highly efficient non-viral transfection system is one of the objectives of future

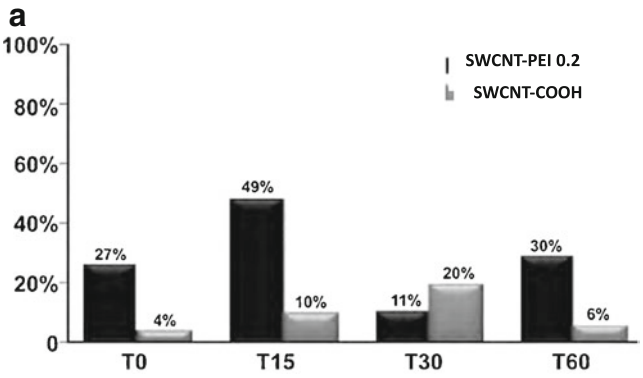

b Size and Zeta (ζ) potential of PLGA–PEI nanoparticles with different PLGA–PEI ratios and PEI–DNA ratios

PEI–DNA ratio	PLGA–PEI ratio 25:1		PLGA–PEI ratio 10:1	
	Size (nm)	ζ potential (mV)	Size (nm)	ζ potential (mV)
Not loaded	211 ± 8	51.1 ± 5.6	231 ± 12	58.8 ± 4.0
5:1	207 ± 11	52.3 ± 8.3	224 ± 10	53.5 ± 4.7
3:1	209 ± 10	48.5 ± 2.6	221 ± 7	53.5 ± 4.0
2:1	211 ± 9	46.9 ± 3.7	224 ± 9	49.1 ± 0.5
1:1	207 ± 10	42.9 ± 1.7	230 ± 26	46.1 ± 2.8
0.5:1	209 ± 16	36.0 ± 1.9	219 ± 13	32.1 ± 6.7

Values are mean averages ± SD of four different batches of particles.

Fig. 4 HAV adsorption on SWNT–PEI and SWNT–COOH after different contact times

medicine. Nimesh et al., in 2006, and Chen et al., in 2007 (both cited in Ref. [30, 31]) have shown efficient SWNT-mediated transfection of genes, proteins, and nucleic acids into mammalian cells. Nanotubes have great therapeutic potential because of their physical and chemical features and their ability to be activated for ad hoc uses. SWNTs have been evaluated as possible vectors for in-vivo and in-vitro delivery of genes, and proteins; however, to act as vectors, activation is necessary (Ref. [30, 31] and references cited therein). Two sets of activated SWNTs were analyzed: SWNT–COOH and SWNT–PEI. The ability to complex with whole viruses was demonstrated, leading to the possibility of delivering entire virus particles into non-permissive cells that lack a specific receptor for the virus on the cell membrane. For carboxylated SWNTs adsorption was no higher than 35.7 % of the inoculum for 1 ng SWNTs [30, 31]. Increasing the amount of SWNTs resulted in a progressive decrease in adsorption. This finding may be because enteric viruses, for example hepatitis A, have a superficial negative charge at neutral pH of the suspension media. Therefore, partial electrostatic repulsion between SWNT–COOH and the HAV particles (both of which are negatively charged) might occur. Increasing the amount of SWNTs may increase the repulsion. When the contact time was increased, the amount of adsorption did not increase [30, 31]. This electrostatic interaction is rapid and noticeable for SWNT–PEI but not for SWNT–COOH. Adsorption is higher for SWNT–PEI than for SWNT–COOH. PEI in aqueous solution has a high positive charge density at neutral pH, and this facilitates adsorption of negatively charged viruses. In 1991, Gajardo et al. used PEI to change electronegative glass powder into electropositive glass powder, thus increasing its virus-adsorbing properties (reported in Ref. [30, 31]). In 2004 Bivas-Benita et al. clearly confirmed that the zeta potential of PEI adsorbed at different ratios on poly(*d*,*l*-lactide-co-glycolide)–PLGA polymers is strongly positive (reported in Ref. [30, 31]). The Z potential, on interaction between PEI and virus, was still positive, although to a lesser extent (personal data, as reported in Ref. [30, 31]). In a preliminary set of experiments, no particular differences in adsorption were evident among different SWNT–PEI weight ratios ranging from 1:2.5 to 1:0.5, whereas significant differences were observed among SWNT–PEI 0.5, SWNT–PEI 0.2, and SWNT–COOH. Fischer et al., in 1999, and Nimesh et al., in 2006, both showed that the cytotoxicity of SWNT–PEI depends on the molecular weight and the amount of PEI (reported in Ref. [30, 31]). To reduce cell cytotoxicity and steric hindrance during the infection process, only the 1:0.2 ratio was investigated for future in vivo SWNT–PEI applications. To explain adsorption of the nucleic acid and the excess electropositive charges, Gautam et al., in 2000, calculated that at the 1:0.5 weight ratio using 25 kDa branched PEI, there are more nitrogen groups present on PEI than phosphate groups on DNA (reported in Ref. [30, 31]). In the experiments, the number of nitrogen groups was not calculated but the maximum adsorption was at 1:0.5 with 100 % adsorption with up to 10^4 gen equiv. in the inoculum and 92.5 % with 10^5 gen equiv. in the inoculum (personal data, as reported in Ref. [30, 31]). Unlike SWNTs activated with carboxyl groups, PEI has maximum adsorption at higher concentrations, from 100 μg to 10 ng for SWNT–PEI 0.2 and at 100 μg for SWNT–PEI 0.5. The need for more SWNT–PEI than carboxylate–SWNT may be because of the number of free nitrogen groups on PEI after the interaction with the carboxyl groups. At 1 pg, SWNT–COOH has adsorptive activity twice that of SWNT–PEI [30, 31]. A smaller number of carboxyl groups reduces electrostatic rejection of the virus. With regard to the different concentrations, at each value, SWNT–PEI 0.2 resulted in significantly greater recovery than SWNT–PEI 0.5 or SWNT–COOH.

This is the first study describing the use of SWNTs as carriers of human viruses [30, 31].

New strategies for cleaning deteriorated stone surfaces based on use of carbon nanomicelles as a carrier for cleaning agents

Materials and procedures

Pentelic marbles from the Basilica Neptuni in Rome, Italy, were treated with a homogeneous and stable dispersion of pristine SWCNTs and functionalized carbon nano-fibers (CNFs-COOH). The carbon nanomaterials were dispersed in Tween 20 (3 %, *w*/*w*) and sonicated in an ultrasonic bath for 10 min, to obtain an homogeneous and stable dispersion, [32, 33]. The marble surface was treated with these dispersions by use of an immersion coating procedure. Enzymatic treatment with glucose oxidase (GOD) and lipase were also performed. In the former treatment 5 mL aqueous solution containing GOD enzyme (0.5 $mg\,mL^{-1}$) and 160 $mmol\,L^{-1}$ glucose substrate were applied to the stone surface for 60 min contact time. During the catalytic reaction, the H_2O_2 was measured and then the surface was copiously washed with distilled water (to reach neutrality) to remove residual enzyme and excess H_2O_2 produced. In the latter treatment, the stone samples were coated by immersion in a solution (5 mL) containing lipase enzyme (0.5 $mg\,mL^{-1}$), for a contact time of 7 min, at T=38 °C [32, 33]. The poultice solution was prepared by adding lipase to a carbonate buffer solution (0.1 $mol\,L^{-1}$, pH 8.7) also containing ammonium carbonate (0.1 $mol\,L^{-1}$).

After cleaning, the stone samples were sequentially washed with distilled water and carbonate buffer solution, to remove excess applied lipase enzyme [32, 33].

Results and discussion

Pentelic marbles from the Basilica Neptuni (27–25 BC) show signs of deterioration, which can be identified as black crust and black and grey patina [32, 33]. Four cleaning procedures were used on the marbles, based on nanomicelles containing functionalized nanofibers (CNF-COOH) or pristine SWCNTs and dispersed in Tween 20, or on enzymatic bio-cleaning with glucose oxidase (GOD) or lipase. These were compared with conventional chemical treatment, for example EDTA or Tween 20 aqueous solution, both suspended in a sepiolite micrometric clay.

Infra-red spectra and color measurements were used to evaluate the efficacy of the treatments. The most desirable outcome is the reappearance on the surface of the underlying calcite grains embedded with inner gypsum inclusions.

The best cleaning performance of the four treatments, in terms of removal of the black crust, was that of CNF-COOH-based nanomicelles (Fig. 5a–f; supplementary material Fig. S4 a–f). Pristine SWCNTs are also efficient at removing the black crust, but to a lesser extent. Glucose oxidase (GOD)-based biocleaning is efficient at removing the grey and dark patina, but works slowly on the black crust. The lipase-based cleaning approach is efficient also at black patina removal, although at a working temperature of 38 °C.

The higher efficiency of nano fibers vs. the nanotubes at removing the black crust may be related to the functionalization of the former with carboxylic acid, which gives the fibers hydrophilic character [32, 33]. The presence of COO^- groups at pH 6 on the CNF walls induces an electrostatic barrier, resulting in Coulombic repulsion among the entangled nanofibers, which, consequently, self-assemble as an isolated and separated nano-carrier of the cleaning agent, with a resulting larger surface area. In particular, the higher surface-to-volume ratio implies higher loading capacity of these isolated nano-carriers for the Tween 20 micelles which act as the cleaning agent. The entangled hydrophobic "as deposited" carbon nanotubes have a smaller nominal surface area, with a consequent lower loading capacity of Tween 20 micelles and, in turn, lower cleaning capacity. Conventional chemical treatments, for example Tween 20 aqueous solution and EDTA agent, both suspended in a sepiolite micrometric clay, resulted in a substantially unaltered black crust of thickness comparable with that of the sample before treatment.

The efficacy of the cleaning treatments was assessed by FT-IR studies, performed on the samples before and after the different treatments (Fig. 6). The typical fingerprint of the inner gypsum inclusions in the calcite grain is detected only for the sample treated with CNF-COOH–Tween 20 (Fig. 6b) and is completely absent from the spectra recorded for the samples treated with the SWCNTs–Tween 20 dispersion (Fig. 6a) or with conventional chemical treatments (Fig. 6c). This means that the CNFs-COOH–Tween 20-based poultice has a better cleaning performance and simultaneously maintains the inner tubular gypsum layer, so-called "patina nobile" [32, 33]. In fact, in Fig. 6b the adsorption bands centered at approximately 1100, 670, 595, and 475 cm^{-1} are related to the presence of the "*inner gypsum*" layer, according to the literature reported in Ref. [32, 33]. In addition, several other adsorption bands are labeled in Fig. 6 and supplementary material Fig. S5) and they correspond to the following stretching and bending frequencies: O, calcium oxalate (whewellite, and wedellite, 3400–3600, 1626, 1324, 947, 882, and 779 cm^{-1}; typical frequencies of the dihydrate weddellite are 1640, 1323, and 780 cm^{-1}); C, calcite (1432 and 875 cm^{-1}); A, apatite (CO_3–apatite–dahllite, 1475–1419, 1050–1040, and 600 cm^{-1}); S, silicates (1100 and 475 cm^{-1}), and, finally, H*, hemihydrate anhydrite (3615–3465, 1629, 1158–1100, and 605–667 cm^{-1}).

The FT-IR spectra reported in supplementary material Fig. S5 also show there is no etching damage to the marble substrata after GOD biocleaning performed at 1 h and 12 h, respectively. In addition, no significant evidence of gypsum is detected for the A and B samples upon GOD treatment, as is the case for CNFCOOH–Tween 200-based bio-cleaning applied to the black crust. This is probably related to the typical H_2O_2 oxidation mechanism, which is able to oxidize the $CuSO_4.2H_2O$ to peroxydisulfate compounds and probably also gypsum in the grey and dark patina, which is less abundant than in the black crust anyway. The qualitative differences observed after the GOD-based bio-cleaning and the CNF-COOH nanotechnology treatment could be explained considering that the marble samples have low porosity (according to the BET values reported in Ref. [32, 33]) and this could induce the GOD enzyme to catalyze the production of H_2O_2 only on the stone surfaces (avoiding diffusion into the bulk of the marble substrata). According to this hypothesis, a thicker black crust could be not removed, efficiently. Furthermore, the biocide properties of the H_2O_2 could be particularly active toward the biopatina, which is known to be only one aspect of the complex physicochemical composition of the environmental black crust.

Colorimetric measurements were performed with a spectrophotometer in accordance with the procedure described in Ref. [32]; the results are reported in supplementary material Table S2. The best recovery of the initial chromatic properties, which is associated with the smallest values of ΔE^* (the total color difference, as reported in supplementary material Table S2) confirms that the carbon nanomicelles assembled with the CNFs-COOH–Tween 20 together with the GOD bio-cleaning are also the best cleaning agents in

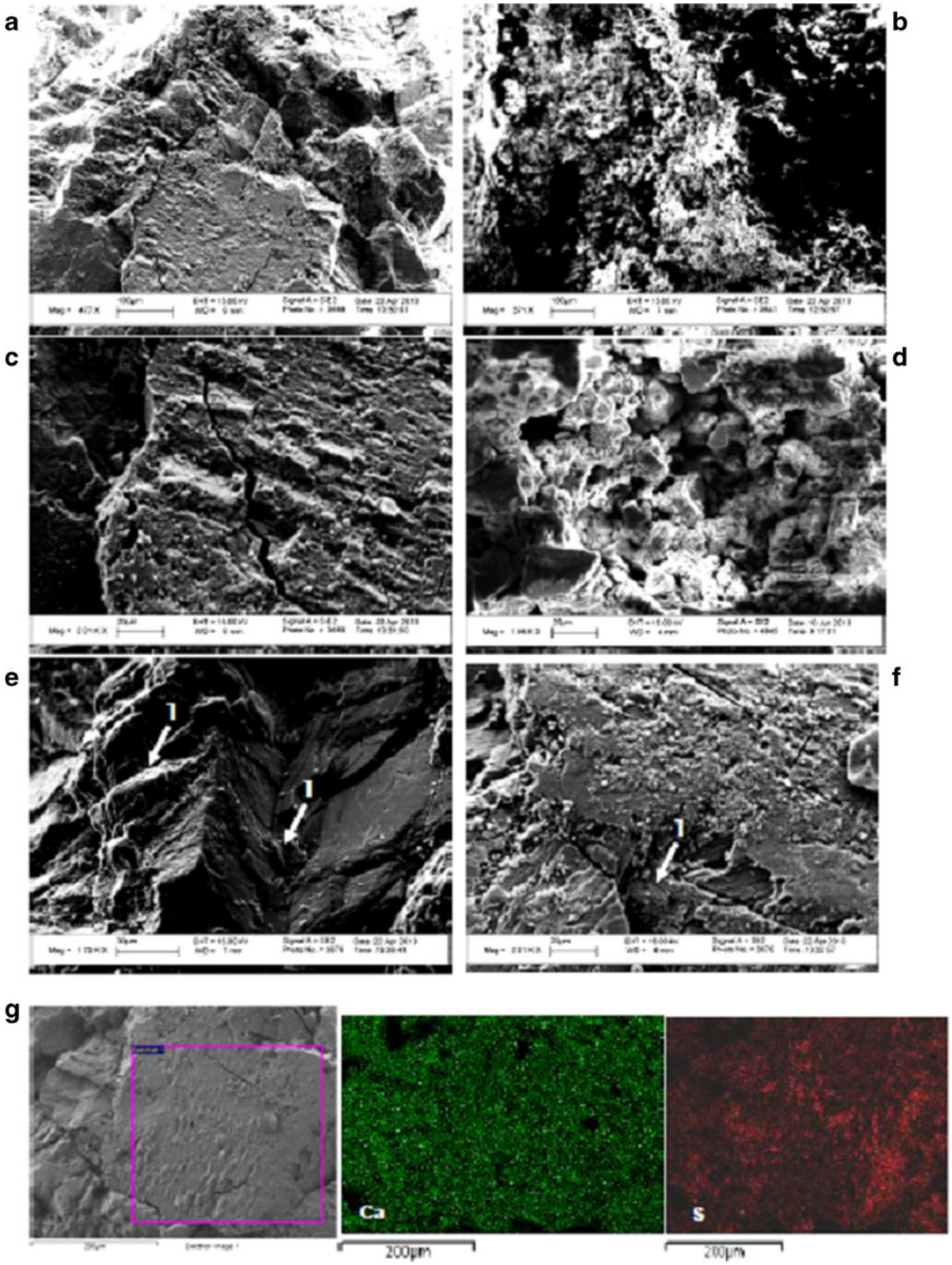

Fig. 5 **a**, **c**: SEM micrographs detected by the secondary electrons (SE) of polished marble (sample C) treated with CNFs-COOH–Tween 20 cleaning agent. **b**, **d**: comparison with the same area of the same sample, before application of the treatment. **e**, **f**: micrographs (SE image) evidence of the tubular crystals of gypsum (*arrow 1*). **g**, EDX distribution maps of Ca and S of the same polished marble area (sample C)

comparison with conventional chemical treatment. These results, demonstrate that these new cleaning strategies based on carbon nano-fibers can efficiently remove the black crust from marble of cultural heritage interest.

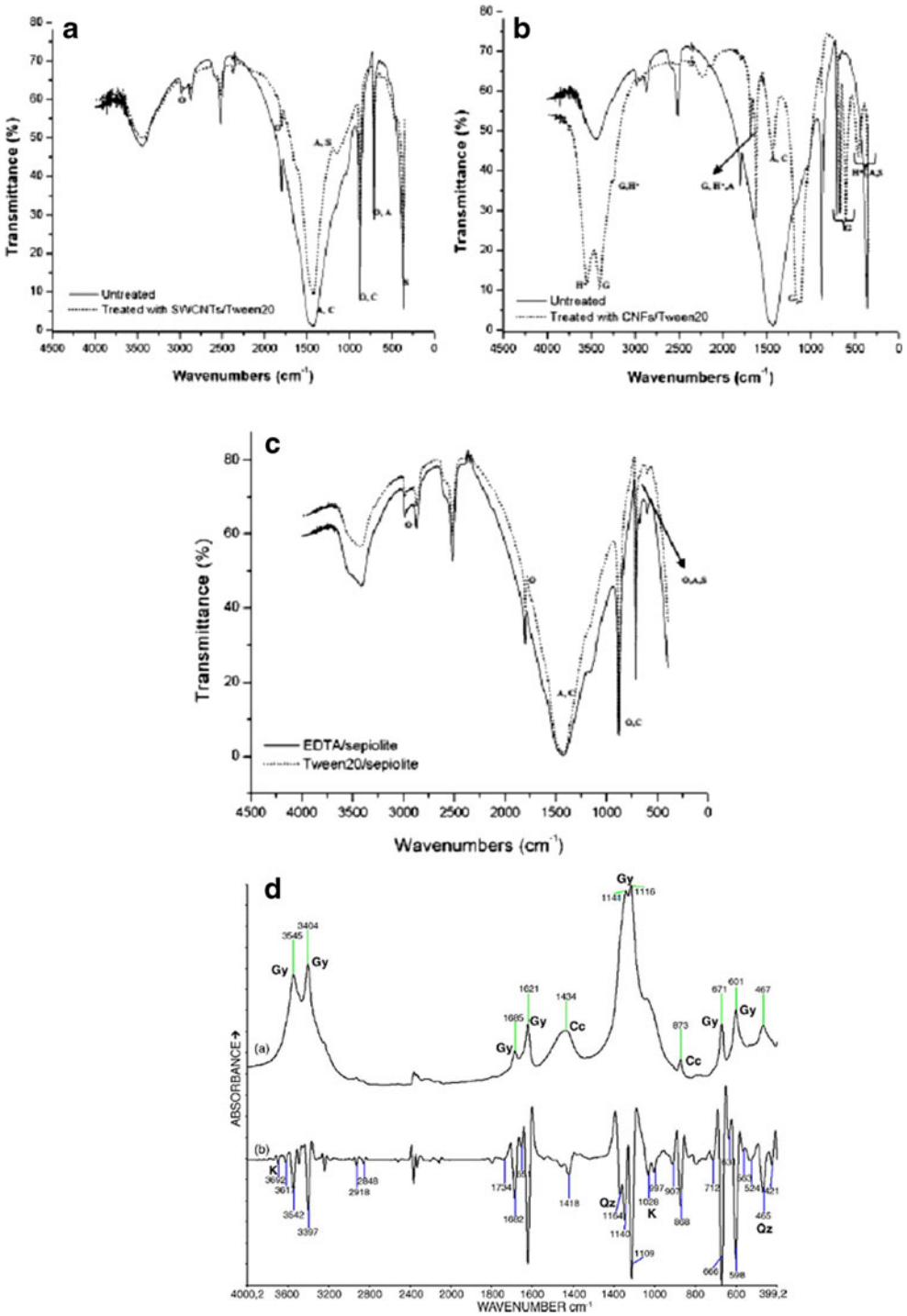

Fig. 6 Comparison of FT-IR spectra obtained from marble sample C before and after the nanotechnology treatment with: **a** Pristine-SWCNTs–Tween 20 nanodispersion and **b** CNFs-COOH–Tween 20 nanomicelles. **c** FT-IR spectra of the same sample, C, treated with EDTA and Tween 20 solution, supported by micrometric sepiolite clay (conventional chemical treatment). FT-IR spectral assignment: O, calcium oxalate (whewellite, and wedellite, 3400–3600, 1626, 1324, 947, 882, and 779 cm^{-1}; typical frequencies of the weddellite dihydrate are 1640, 1323, and 780 cm^{-1}); C, calcite (1432 and 875 cm^{-1}); A, apatite (CO_3-apatite-dahllite, 1475–1419, 1050–1040, and 600 cm^{-1}); G, gypsum (1100, 670, 595, and 475 cm^{-1}); S, silicates (1100 and 475 cm^{-1}), and, finally, H*, hemihydrate anhydrite (3615–3465, 1629, 1158–1100 and, 605–667 cm^{-1})

Assembly of amperometric biosensors modified by carbon nanomaterial–hemin nanocomposite for direct electrochemical detection of an environmental pollutant, nitrite

Materials

A carboxylated carbon nanofiber modified glassy carbon electrode (CNF-COOH–GC) was assembled by using functionalized CNFs previously dispersed in CH_3CN. The resulting suspension, containing 1.0 $mg mL^{-1}$ CNFs, was placed in a ultrasonic bath for 1 h at room temperature. From this homogeneous CNF dispersion, 2 μL was cast on the GC electrode surface and the solvent was left to evaporate at room temperature. Hemin was immobilized on the CNF-modified GC electrode by dipping it into a 3 $mg mL^{-1}$ hemin solution (at pH 5.6 in 0.2 $mol L^{-1}$ acetate buffer) overnight, [34]. The resulting modified electrode is denoted

"CNF/H/GC"-based biosensor. An SWCNT-OH–hemin-modified GC electrode was assembled in the same way, by use of a homogeneous suspension of SWCNT-OH (1 mg mL^{-1}, previously purified and functionalized with KOH [34]) in CH_3CN (after sonication for 1 h). The resulting modified GC electrode is denoted "SWCNT/H/GC"-based biosensor. Amperometric detection of NO_2^- was performed by using the method of successive additions with NO_2^- concentration ranging from 5 to 250 mmolL^{-1}, working at an applied potential of +0.3 V, vs. Ag/AgCl, Cl^-. Measurement of NO_2^- implies a direct electron transfer-based mechanism which has been widely described in the literature for several protein redox functions [34]. For the amperometric calibration curve for H_2O_2, the same analytical approach as described for NO_2^-, is used, working at an applied potential of 0.0 V, vs. Ag/AgCl (as reference electrode) with the H_2O_2 concentration ranging from 0.05 to 5 mmolL^{-1}.

Results and discussion

Nitrite is one of the most important analytical compounds to investigate because it is a dangerous environmental pollutant. This is probably related to its growing use as fertilizer, detergent, and stabilizing and aromatizing agent in food technology. Hence, its monitoring in water samples and food matrices is extremely important for detection of serious pollution, some of which might be particularly dangerous to human health and cause, for instance, the "blue baby syndrome" in children [34]. Electrochemical oxidation of nitrite requires a high over potential, implying that this process is not spontaneous on bare electrodes. Several strategies, using several types of modified electrode, have been developed to catalyze the nitrate/nitrite redox reaction. Carbon nanomaterials could be a valid alternative for electrode modification. In this section, a study is presented on a carboxylated carbon nanofibers (CNF-COOH)-modified glassy carbon (GC) electrode. The calibration plot is shown in Fig. 7, and all the analytical data are reported in supplementary material Table S3. Compared with previous work [34] better results were obtained with a CNF/H/GC third-generation biosensor (based on a hemin direct electrochemistry mechanism) in terms of extended linearity, higher sensitivity, good reproducibility, short response time, and lower detection limit. In addition, application of +0.30 V as working potential, instead of +0.90 V (oxidizing potential at non-modified conventional electrodes), for the amperometric detection of nitrite [34] reduces potential oxidant interferences. Perm-selectivity tests were also performed on possible interference by residues of ascorbic acid (AA), uric acid (UA), and acetaminophen (Ac), the most common interferences in biosensor characterization studies [34]. Value obtained were 50 % for ascorbic acid (AA), 45 % for uric acid (UA), and 38 % for acetaminophen (Ac). Such values

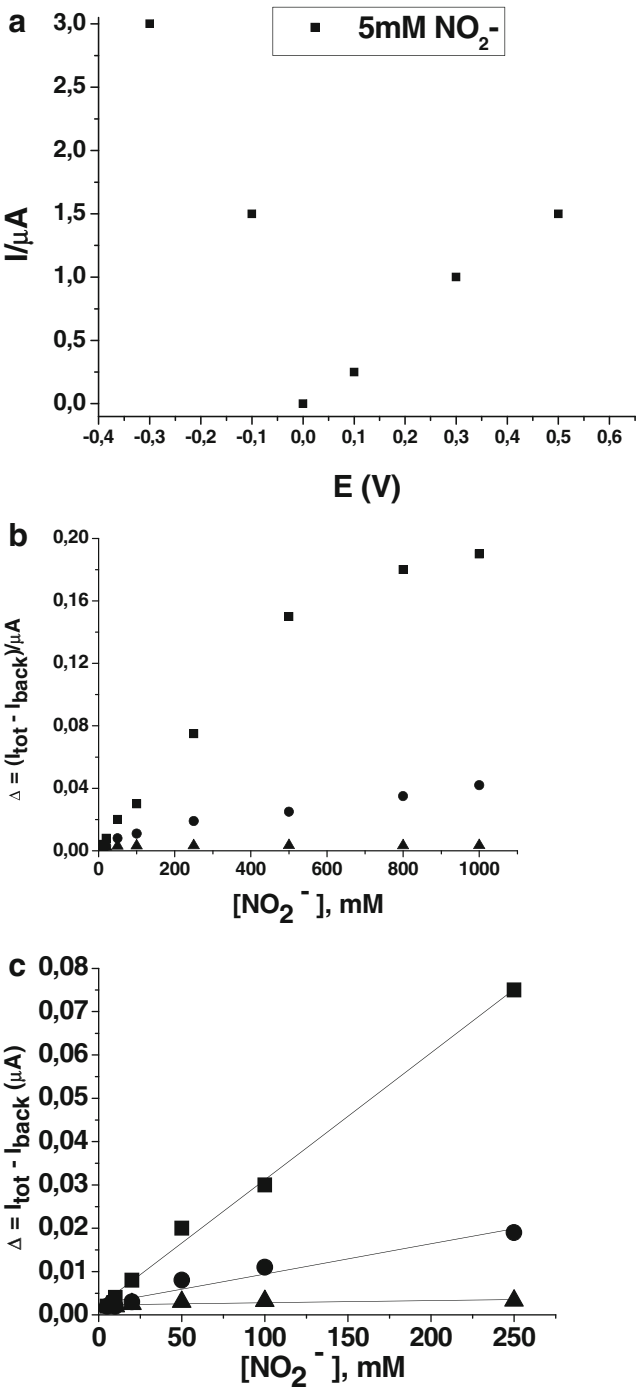

Fig. 7 **a** Hydrodynamic voltammograms obtained from 5 mmolL^{-1} H_2O_2 at CNF/H/GC, performed from −0.3 to +0.3. **b**. Calibration curves at GC (*squares*), CNF/GC (*triangles*), and CNF/H/GC (*circles*) for different concentrations of H_2O_2 from 0.05 to 5 mmolL^{-1}, performed by amperometry at 0.0 V as applied potential vs. Ag/AgCl as reference electrode. **c** Inset plot: calibration plot for H_2O_2 in the linear range (0.05–1 mmolL^{-1})

guarantee a non-compromised signal-to-noise ratio. The calibration plot had a typical Michaelis–Menten profile for NO_2^- concentrations higher than 250 mmolL^{-1} [34]. The apparent Michaelis–Menten constant (K_M^{app}) related to

protein–electrode affinity, can be evaluated from the electrochemical Lineweaver–Burk equation [34], and is 0.44± 0.01 mmolL^{-1} for the CNF/H/GC biosensor. This value is lower than those described in the literature for other NO_2^- biosensors [34], indicative of higher affinity of this sensor for the substrate.

Finally, electrocatalytic activity in H_2O_2 reduction was also demonstrated for both sensors but better results were observed by use of the CNF/hemin/GC-modified electrode, as reported in supplementary material Fig. S6 and Table S4 (for quantitative analytical data) [34]. The best working potential for H_2O_2 amperometric measurements was 0.0 V (selected by use of an hydrodynamic voltammetric study, shown in supplementary material Fig. S6) because of a high signal-to-noise ratio. One of the most important advantages of detection of H_2O_2 at this low potential is minimization of interference effects, as reported above. The possibility of working at 0.0 V also minimizes oxygen electrochemical reduction, which occurs at −0.3 and −0.1 V, also catalyzed by the presence of hemin [34]. When the H_2O_2 concentration was higher than 1 mmolL^{-1}, a typical Michaelis–Menten kinetic profile was observed at CNF/H/GC and SWCNT/H/GC-based biosensors (supplementary material Fig. S6). The apparent Michaelis–Menten constant (K_M^{app}), related to both enzymatic affinity and the ratio of microscopic kinetic constants, can be evaluated (as described above), resulting in a value of 2.6±0.1 mmolL^{-1} for the CNF/H/GC-modified electrode, lower than that calculated for the SWCNT/H/GC biosensor (4.3±0.2 mmolL^{-1}). Compared with other systems described in the literature [34] the K_M^{app} value obtained for the CNF/H/GC biosensor was lower, meaning that a greater affinity for H_2O_2 was achieved (useful for glucose electrochemical biosensor assembly).

Conclusions

This review describes how carbon nanostructured materials are highly performing and useful for several analytical applications. The toxicity of nanomaterials has been demonstrated but only by exposing healthy animals; however, epidemiological studies clearly indicate that cardiac autonomic disturbances linked to particulate exposure are much more likely in people with pre-existing cardiovascular disorders. Concerning this, it is important to evaluate arterial baroreflex control of sinus node as index of cardiovascular autonomic control, because it has been largely implicated as an important negative prognostic index in predicting mortality for ischemic heart disease and myocardial infarction. Because of these considerations it would be desirable to perform studies to evaluate possible alteration of cardiovascular autonomic regulation and, in particular, of arterial baroreflex function, in experimental models of ischemic heart disease.

When carbon nanotubes are coated (of their surfaces, walls, and edges) with biopolymers, this chemical modification makes them highly biocompatible and useful for applications as carriers of genes, DNA, viruses, and drugs for in-vitro and in-vivo studies. Successful binding of an enteric virus (the hepatitis A virus) to activated nanotubes has been demonstrated. The possibility of binding and introducing a virus into a non-permissive cell line to aid viral replication will lead to better understanding of the molecular biology of the virus and a better way to evaluate the in-vivo and/or in-vitro evolution of infection. Furthermore, it will help to provide sufficient amounts of virus to produce protective vaccines against non-replicating viruses. Single-wall carbon nanotubes can also be used to remove viruses from various environmental matrices.

The surface physicochemical properties of nano-micelles have resulted in an innovative method for cleaning, restoration and consolidation of deteriorated historical surfaces in cultural heritage. In particular, results show that nanotechnology and enzyme-based treatments enabled successful removal of black crusts from the altered marble substrata, for example the Basilica Neptuni in Rome, Italy (27–25 BC), especially a cleaning strategy based on functionalized carbon nanofibers. However, feasibility and performance in respect of cleaning efficiency should be quantitatively evaluated on a case-by-case basis. The number of applications and overall treatment time must be evaluated considering different factors, for example the chemical composition, thickness, and uniformity of the black crust, which can vary substantially depending on the material, location, climate, and atmospheric pollution, as widely described in literature by (C. S.-Jimenez 1993). In particular, the nanotechnology proposed here seems to be suitable for deteriorated limestone, and conveniently integrates traditional chemical methods with GOD–lipase-based poultices by use two approaches. First, after consistent removal of the superficial thick black crust, chemical treatment can then follow for more complete decontamination of inner decay products. Second, nanotechnology could be used as the final cleaning method. It would be able to offer the advantageous possibility of removing resistant dark patinas, unaffected by traditional reagents which would, otherwise, would require excessive and unacceptable extreme chemical conditions.

Finally, the biocompatibility of nanostructured materials is of great advantage for immobilizing enzymes, proteins, and antibodies for assembly of biosensors and immunosensors for use with amperometric and/or electrochemical detection. A new functionalized carbon nanomaterial (i.e. carbon nanofibers) has been used to immobilize hemin on a GC electrode surface by use of a simple and reproducible procedure (drop-coating). The best electroanalytical performance obtained with a CNF/H/GC biosensor was compared with that of a SWCNT/H/GC biosensor; this revealed that

the open structure of CNFs combined with their higher surface functional group density were responsible for a beneficial effect on hemin catalytic activity, primarily related to strong covalent protein immobilization (absorption). Investigation of the effect of pH revealed that a quasi-reversible electrochemical profile involving one proton and one electron redox process occurred at the CNF/H/GC biosensor. In addition, greater reversibility was recorded at this modified electrode, as confirmed by electrochemical data and the higher value of the heterogeneous electron-transfer rate constant. Moreover, for the first time, as far as we are aware, the H_2O_2 and NO_2^- electrocatalytic effect observed at a CNF/H/GC-based biosensor has been reported; good analytical performance was obtained in terms of extended linearity, lower detection limit, high sensitivity, significant reproducibility, and short response time.

Acknowledgments The authors wish to thank Professor A. Pietroiusti, Department of Occupational Medicine at the University of Rome Tor Vergata, and Professor M. Divizia, Department of Hygiene and Public Health, at the same University of Rome (Italy) for medical assistance and technical support. The authors also thank Professor C.S. Salerno, Central Institute for Restoration (ICR) of Rome, for collecting deteriorated marble samples and useful discussion.

References

1. Guiseppi-Elie A, Lei C, Baughman RH (2002) Nanotechnology 13:559
2. Yokoyama A, Sato Y, Nodasaka Y, Yamamoto S, Kawasaki T, Shindoh M, Kohgo T, Akasaka T, Uo M, Watari F, Tohji K (2005) Nano Letters 5(1):157–161
3. Qiu X, Freitag M, Perebeinos V, Avouris P (2005) Nano Lett 5:749–752
4. Ferrari M (2005) Nat Rev Cancer 5:161–171
5. Ferriera L, Karp JM, Nobre L, Langer R (2008) Cell Stem Cell 3:136–146
6. Rivera GP, Oberdörster G, Elder A, Puntes V, Parak WJ (2010) ACS Nano 4:5527–5531
7. Sanchez VC, Pietruska JR, Miselis NR, Hurt RH, Kane AB (2009) Wiley Interdiscip Rev Nanomed Nanobiotechnol 1:511–529
8. Kagan VE, Tyurina YY, Tyurin VA, Konduru NV, Potapovich AI, Osipov AN, Kisin ER, Schwegler-Berry D, Mercer R, Castranova V et al (2006) Toxicol Lett 165:88–100
9. Pulskamp K, Diabat S, Krug HF (2007) Toxicol Lett 168:58–74
10. Bottini M, Bruckner S, Nika K, Bottini N, Bellucci S, Magrini A, Bergamaschi A, Mustelin T (2006) Toxicol Lett 160:121–126
11. Sato Y, Yokoyama A, Shibata K, Akimoto Y, Ogino S, Nodasaka Y, Kohgo T, Tamura K, Akasaka T, Uo M et al (2005) Mol Biosyst 1:176–182
12. Poland CA, Duffin R, Kinloch I, Maynard A, Wallace WA, Seaton A, Stone V, Brown S, Macnee W, Donaldson K (2008) Nat Nanotechnol 3:423–428
13. Fenoglio I, Tomatis M, Lison D, Muller J, Fonseca A, Nagy JB, Fubini B (2006) Free Radical Biol Med 40:1227–1233
14. Fenoglio I, Greco G, Tomatis M, Muller J, Raymundo-Pinero E, Beguin F, Fonseca A, Nagy JB, Lison D, Fubini B (2008) Chem Res Toxicol 21:1690–1697
15. Muller J, Huaux F, Fonseca A, Nagy JB, Moreau N, Delos M, Raymundo-Pinero E, Beguin F, Kirsch-Volders M, Fenoglio I et al (2008) Chem Res Toxicol 21:1698–1705
16. Fubini B, Ghiazza M, Fenoglio I (2010) Nanotoxicology 4:347–363
17. Shvedova AA, Kisin ER, Porter D, Schulte P, Kagan VE, Fadeel B, Castranova V (2009) Pharmacol Ther 121:192–204
18. Lacerda L, Bianco A, Prato M, Kostarelos K (2006) Adv Drug Delivery Rev 58:1460–1470
19. Jiang W, Kim BY, Rutka JT, Chan WC (2008) Nat Nanotechnol 3:145–150
20. Verma A, Stellacci F (2010) Small 6:12–21
21. Singh R, Pantarotto D, Lacerda L, Pastorin G, Klumpp C, Prato M, Bianco A, Kostarelos K (2006) Proc Natl Acad Sci USA 103:3357–3362
22. Shubayev VI, Pisanic TR, Jin S (2009) Adv Drug Del Rev 61:467–477
23. Liu Z, Robinson JT, Sun X, Dai H (2008) J Am Chem Soc 130 (33):10876–7
24. Sun X, Liu Z, Welsher K, Robinson JT, Goodwin A, Zaric S et al (2008) Nano Res 1(3):203–212
25. Yang X, Zhang X, Liu Z, Ma Y, Huang Y, Chen Y (2008) J Phys Chem C 112(45):17554–8
26. Bianco A, Kostarelos K, Prato M (2005) Curr Opin Chem Biol 9 (6):674–9
27. Legramante JM, Valentini F, Magrini A, Palleschi G, Sacco S, Iavicoli I, Pallante M, Moscone D, Galante A, Bergamaschi E, Bergamaschi A, Pietroiusti A (2009) Hum Exp Toxicol 28 (6–7):369–375
28. Pietroiusti A, Massimiani M, Fenoglio I, Colonna M, Valentini F, Palleschi G, Camaioni A, Magrini A, Siracusa G, Bergamaschi A, Sgambato A, Campagnolo L (2011) ACSNano 5(6):4624–4633
29. Cicchetti R, Divizia M, Valentini F, Argentin G (2011) Toxicology in Vitro 25:1811–1819
30. Petrinca AR, Donia D, Cicchetti R, Valentini F, Argentin G, Carbone M, Pietroiusti A, Magrini A, Palleschi G, Divizia M (2010) Journal of Virological Methods 168:1–5
31. Carbone M, Valentini F, Caminiti R, Petrinca AR, Donia D, Divizia M, Palleschi G (2010) Biomed Mater 5(3):35001
32. Valentini F, Diamanti A, Palleschi G (2010) Applied Surface Science 256(22):6550–6563.
33. Valentini F, Diamanti A, Carbone M, Bauer EM, Palleschi G (2012) Applied Surface Science 258(16):5965–5980
34. Valentini F, Cristofanelli L, Carbone M, Palleschi G (2011) Electrochim Acta (December 2011). doi:10.1016/j.electacta.2011.12.027